

HIGHER-ORDER QCD CORRECTIONS TO HIGGS BOSON TRANSVERSE-MOMENTUM DISTRIBUTION

Fabrizio Caola

Rudolf Peierls Centre for Theoretical Physics, Oxford University, Oxford, UK

Kirill Kudashkin

Department of Physics, University of Milan, Milan, Italy

Jonas M. Lindert

Department of Physics and Astronomy, Sussex University, Falmer, UK

Kirill Melnikov

Institute for Theoretical Particle Physics (TTP), KIT, Karlsruhe, Germany

Pier F. Monni

Theoretical Physics Department, CERN, Geneva, Switzerland

Lorenzo Tancredi

Rudolf Peierls Centre for Theoretical Physics, Oxford University, Oxford, UK

Chris Wever

Physik-Department T31, Technische Universität München, Garching, Germany

Abstract

We present up-to-date Standard Model theory predictions for the Higgs transverse-momentum (p_\perp) distribution. In the region of intermediate values of transverse momenta we present the NNLL+NLO QCD predictions including both top and bottom quark contributions. At very large $p_\perp \gg 2m_t$ we show the next-to-leading order QCD corrections to the production of the Higgs boson at the LHC.

1 Introduction

Detailed exploration of the Higgs boson is one of the central tasks of the particle physics program at the LHC. Since the majority of the Higgs bosons is produced by gluon fusion, it is only natural to study Higgs coupling to gluons as precisely as possible. Incidentally, the Higgs-gluon coupling is very interesting phenomenologically. Indeed, since the Higgs coupling to gluons is loop-induced, and since contributions of heavy particles whose masses are generated by the Higgs mechanism do not decouple, the ggH interaction vertex becomes an intriguing probe of the TeV-scale physics. The goal of this proceeding is to present the Higgs p_\perp spectrum in the moderate ¹⁾ $m_b \lesssim p_\perp \lesssim m_H$ as well as the large ²⁾ $p_\perp \gg 2m_t$ range.

In the moderate p_\perp range we present results that involve the top and bottom-quark contributions at next-to-leading order combined with next-to-next-to-leading logarithmic transverse momentum resummation (NLO+NNLL), presented originally in Ref. ¹⁾. Although the contributions of bottom and charm loops to the ggH coupling and direct production of a Higgs boson in quark fusion $q\bar{q} \rightarrow H$, $q \in \{c, b\}$ are small in the Standard Model, if the Yukawa couplings differ from their Standard Model values, these light-quark effects in Higgs production become much more important. In fact, it was pointed out in Refs. ^{3, 4)} that studies of kinematic distributions of Higgs bosons produced in hadron collisions may lead to interesting constraints on light quark Yukawa couplings, especially at the high-luminosity LHC.

On the other hand, to disentangle the effective one-loop ggH coupling induced through heavy BSM particles from that induced through the SM top quark running in the loop, one has to consider the Higgs boson transverse momentum distribution at very large Higgs p_\perp .⁵⁾ The two-loop amplitudes for the production of the Higgs boson at high- p_\perp were computed in Ref.⁶⁾ and enabled the calculation of the Higgs boson transverse momentum distribution for $p_\perp > 2m_t$ at NLO QCD presented originally in Ref.²⁾, that we report in the second half of the proceedings.

2 Results

We discuss here our main result for the Higgs transverse momentum distribution. We separate the discussion for the case where the Higgs transverse momentum is below and above the top-mass threshold, i.e. $p_\perp \sim 2m_t \sim 350$ GeV. In section 2.1, results are shown for moderate $p_\perp \lesssim 100$ GeV values, while in section 2.2 our results for very large $p_\perp \gtrsim 350$ GeV values are presented. We refer to Refs.^{1, 2)} for the details of the computations.

2.1 Higgs transverse-momentum distribution below the top-mass threshold

Our results for the fixed-order and matched distributions below the top-mass threshold are shown in Fig. 1. Let us consider first the left plot that shows our result for the top-bottom interference contribution. In order to make a conservative estimate of the uncertainty for the matched interference distribution we took the envelope of the following uncertainties: the usual scale variations of μ_R, μ_f ; the variation of half and twice the central scale $Q_t = Q_b = m_H/2$ at fixed central scales $\mu_R = \mu_f$; the difference between the on-shell and $\overline{\text{MS}}$ bottom-mass scheme; matching scheme difference between additive and multiplicative cases; finally the difference between resummation scale choice of $Q_b = 2m_b$ and $Q_b = m_H/2$. The effect of the resummation in this case is larger than in the full spectrum shown in the right plot, as was already observed in Fig. 1 of Ref.⁸⁾. The qualitative features of the fixed order result are unchanged by the resummation, which however has a noticeable effect. The resummation prescription tames the fixed order result down to $10 \text{ GeV} \lesssim p_\perp$, while at the same time keeping the errors under control at the order of at most $\sim 20\%$ throughout the range of $10 \text{ GeV} \lesssim p_\perp \lesssim 70 \text{ GeV}$.

In the right plot of Fig. 1 we present our main results for the full spectrum. The plot shows the fixed-order result in orange and the total top and bottom resummed result in blue. The uncertainty band for the resummed result contains in this case only the scale variations of μ_R, μ_f and $Q_t = Q_b$, since as we have seen above the effects of the bottom-mass scheme and different resummation scales for the bottom are already well captured by these variations. At large values of the Higgs $p_\perp \gtrsim 40$ GeV, the fixed-order result is contained in the error band of the resummed result. However, at smaller values $p_\perp \lesssim 40$ GeV, we observe a marked difference between the two results. The error for the full matched result is well under control and contained to about 5-10% in this range, increasing to about $\sim 20\%$ at larger p_\perp , where the effect of the resummation prescription is reduced and the fixed order NLO result is approached. At the same time, the effect of the bottom contribution on the central value is small though still noticeable, while its effect on the error-band widths is negligible.

This final result constitutes the best theoretical prediction up till now for the Higgs transverse momentum distribution for moderate values of the Higgs p_\perp and is to be compared with current experimental measurements. From our discussion above it becomes clear that further improvement of our results is appreciated in the region of Higgs $p_\perp \gtrsim m_h/2$, where the collinear approximation breaks down and the resummation is turned off. This improvement would require matching to higher fixed-order NNLO result.

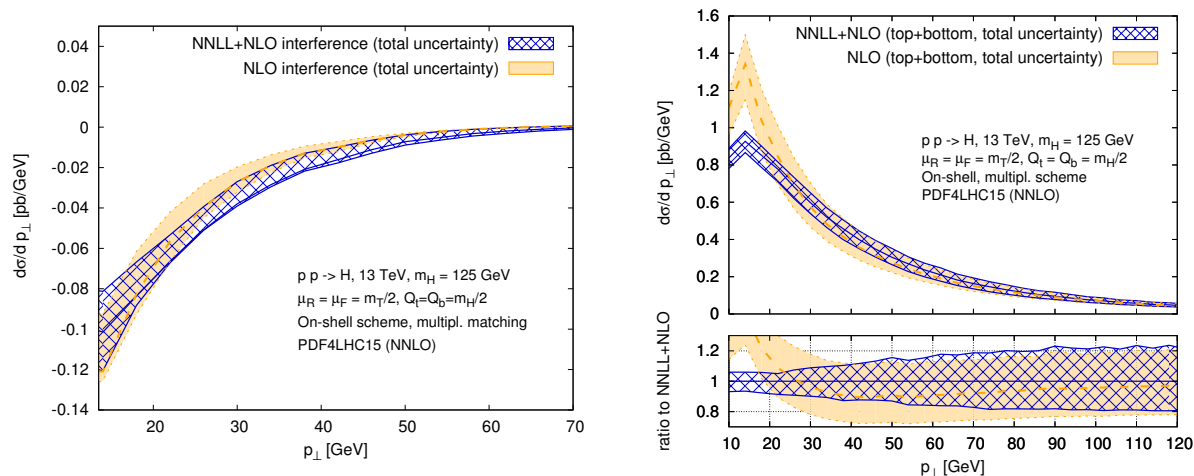


Figure 1: The distributions for the top-bottom interference contribution (left) and the full NNLL matched result (right), using the multiplicative scheme with resummation scale $Q_b = Q_t = m_h/2$ as central values. See text for details.

2.2 Higgs transverse momentum distribution at very large p_\perp

For the results in this range we use the amplitudes in Ref. ⁶⁾ expanded in the small ratio $4m_t^2/p_\perp$, keeping sub-leading terms in the expansion. We start by illustrating how well our mass expansion of the amplitude works at LO. In the left plot of Fig. 2, we compare the exact leading-order p_\perp distribution of the Higgs boson with its various expansions. We see that the amplitude expanded to $\mathcal{O}(m_H^0, m_t^2)$ terms gives the result that tracks the leading-order amplitude all the way down to the top-quark threshold; on the contrary, if the sub-leading top-quark mass terms are not retained, the expanded and exact cross sections have $\mathcal{O}(20\%)$ difference at $p_\perp \sim 800$ GeV.

We employ the five-flavor scheme and consider the bottom quark as a massless parton in the proton. We use the NNPDF3.0 set of parton distribution functions ⁹⁾ at the respective perturbative order and employ the strong coupling constant α_s that is provided with these PDF sets. We choose renormalization and factorization scales to be equal and take as the central value

$$\mu_0 = \frac{H_T}{2}, \quad H_T = \sqrt{m_H^2 + p_\perp^2} + \sum_j p_{\perp,j}. \quad (1)$$

The inclusive cross sections are computed for both the point-like Higgs-gluon coupling, obtained by integrating out the top quark, and for the physical Higgs-gluon coupling with a proper dependence on m_t . We will refer to the two cases as HEFT and SM, respectively.

The Higgs-boson transverse-momentum distribution for $p_\perp > 350$ GeV is shown in the right plot of Fig. 2. The results show that both the SM and the HEFT K -factors are flat over the entire range of p_\perp . For the central scale $\mu = \mu_0$ (see Eq. (1)), the differences between the two K -factors is about 5%. The scale dependence of HEFT and SM results are also similar. The residual theoretical uncertainty related to perturbative QCD computations remains at the level of 20%, as estimated from the scale variation. Such an uncertainty is typical for NLO QCD theoretical description of many observables related to Higgs boson production in gluon fusion. Further improvements in theory predictions are only possible if the proximity of the HEFT and SM K -factors is taken seriously and postulated to occur even at higher

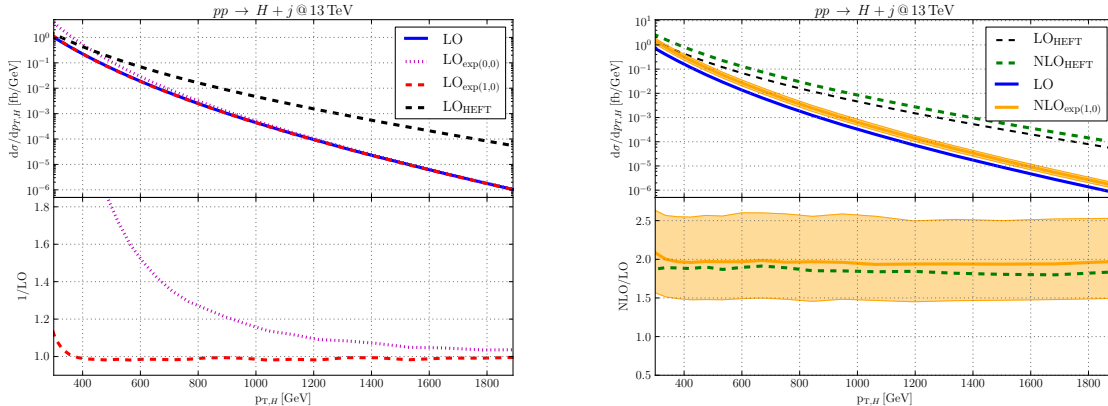


Figure 2: Left: Ratio of approximate to exact leading order cross sections. By retaining $\mathcal{O}(m_t^2/p_\perp^2)$ corrections in scattering amplitudes (red line), we obtain an excellent approximation to the exact LO result. Right: Transverse momentum distribution of the Higgs boson at the LHC with $\sqrt{s}=13$ TeV. The upper panel shows absolute predictions at LO and NLO in the full SM and in the infinite top-mass approximation (HEFT). The lower panel shows respective NLO/LO correction factors. The bands indicate theoretical errors of the full SM result due to scale variation.

orders. In this case, one will have to re-weight the existing HEFT $H + j$ computations^{10, 11, 12)} with the exact leading-order cross section for producing the Higgs boson with high p_\perp . In fact, such a reweighting can now be also performed at the NLO level.

3 Summary

We presented accurate theory predictions to the Higgs boson transverse momentum distribution. In the region of intermediate values of transverse momenta, $m_b \lesssim p_\perp \lesssim m_H$, we presented a description of the Higgs p_\perp spectrum at NNLL+NLO QCD including both top and bottom quark contributions. We found that the uncertainty on the top-bottom interference is $\mathcal{O}(20\%)$ in the region of interest $m_b \lesssim p_\perp \lesssim m_H$. Given the intrinsic ambiguities from scale dependence and, in particular, from the choice of the bottom-mass renormalization scheme and matching scheme, any improvement in this description will inevitably require the computation of the NNLO QCD corrections to the bottom-quark contribution to $gg \rightarrow H$ and $gg \rightarrow H + jet$.

In the range of very large p_\perp values, we presented the NLO QCD corrections to the Higgs boson transverse momentum distribution. To compute them, we employed the calculation of the two-loop scattering amplitudes for all relevant partonic channels⁶⁾ where an expansion in m_t/p_\perp was performed. The real-emission corrections were computed with the `OpenLoops`⁷⁾ program. We have found that the QCD corrections to the Higgs-boson transverse-momentum distribution increase the leading order result by almost a factor of two. However, their magnitude appears to be quite similar to the QCD corrections computed in the approximation of a point-like Higgs-gluon vertex; the difference of the two result is close to 5%. Our computation removes the major theoretical uncertainty in the description of the Higgs boson transverse momentum distribution at high p_\perp and opens a way to a refined analysis of the sensitivity of this observable to BSM contributions, using existing¹³⁾ and forthcoming experimental measurements.

References

1. F. Caola, J. M. Lindert, K. Melnikov, P. F. Monni, L. Tancredi and C. Wever, JHEP **09** (2018) 035.
2. J. M. Lindert, K. Kudashkin, K. Melnikov and C. Wever, Phys. Lett. B **782** (2018) 210.
3. F. Bishara, U. Haisch, P. F. Monni and E. Re, Phys. Rev. Lett. **118** (2017) 121801.
4. Y. Soreq, H. X. Zhu and J. Zupan, JHEP **12** (2016) 045.
5. C. Arnesen, I. Z. Rothstein and J. Zupan, Phys. Rev. Lett. **103** (2009) 151801.
6. K. Kudashkin, K. Melnikov, and C. Wever, JHEP **02** (2018) 135.
7. F. Cascioli, P. Maierhöfer and S. Pozzorini, Phys. Rev. Lett. **108**, 111601 (2012).
8. A. Banfi, P. F. Monni and G. Zanderighi, JHEP **01** (2014) 097.
9. R. D. Ball *et al.* [NNPDF Collaboration], JHEP **1504**, 040 (2015).
10. R. Boughezal *et al.*, Phys. Rev. Lett. **115** (2015) no.8, 082003.
11. R. Boughezal, C. Focke, W. Giele, X. Liu and F. Petriello, Phys. Lett. B **748** (2015) 5.
12. X. Chen, T. Gehrmann, E. W. N. Glover, and M. Jaquier, Phys. Lett. B **740** (2015) 147.
13. CMS Collaboration, (2017) CMS-PAS-HIG-17-010.